A study of high-performance sensing behavior of biosensor based on photonic crystal

SUMMARY

Dissertation

Submitted for the Award of the Degree

of

Master of Philosophy

In

Physics

Submitted By

Mohit Kumar

Enrolment No. 553/18

Under the supervision of

Dr. Khem Bahadur Thapa

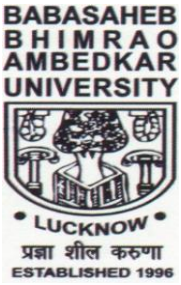

Department of Physics

School of Physical & Decision Science

Babasaheb Bhimrao Ambedkar University (A Central University)
Lucknow – 226025, (U.P.) INDIA

June 2022

SUMMARY

In optics, the velocity of propagation v of the light in a medium of permittivity ε and permeability μ is simply given by Maxwell's equations [1,2,3]

$$n = \frac{c}{v} = \sqrt{\epsilon_r \, \mu_r} \quad (1)$$

For the non-magnetic medium, the relative permeability is one i.e. μ_r=1, therefore the refractive for dielectric medium is;

$$n = \sqrt{\epsilon_r} \quad (2)$$

$$n^2 = \epsilon_r \quad (3)$$

Now, such dielectrics are arranged in a periodic manner, then the periodic dielectric structure can interact resonantly with radiation with a wavelength equal to the periodicity length of the dielectric lattice, called a photonic crystal. Such periodic structure can affect the properties of photons in much the similar way that conductor and ordinary semiconductors crystals affect the properties of electrons. We can say that the photonic crystal materials have periodically modified refractive index and exhibit photonic bandgap. When the electromagnetic wave (EMW) propagates in the photonic crystal, the EMW cannot propagate from it called a forbidden band gap. Due to the existence of the band gaps, the PCs have several applications such as optical sensors, biosensors, switches, reflectors, optical filters, etc. [4,5].

The biosensors based on long range surface plasmon resonance (LRSPR) are used in the detection of biological macromolecules and even cell structure because it has a lower loss, longer propagation distance, and deeper penetration depth of surface plasmon polaritons. In the LRSPR sensing medium, variation in the concentration of biomolecules yields a local change in the refractive index in contact of the metal surface. The modified optical density leads to a variable diffusion constant of the SPP and can alternatively be measured by the attenuated total reflection technique. The TM polarized surface plasmon wave is excited by a metal thin film, however, the long-range surface plasmon resonance (LRSPR) based prism with metal-dielectric interfaces is embedded in the intermediate layers [6].

Since many representative studies have been done based on the LRSPR and described to achieve high analysis accuracy for the application of long-range geometry SPR sensor [7]. However, the demand and development of high durability with maximum sensitivity, better detection accuracy (DA) and more optimized LRSPR based sensors are growing in this field of interest from last few couple of years. In the conventional LRSPR based sensors, Gold (Au) is implemented as the metal constituent, but it is not able to process oxidation, additionally, it also does not react with utmost chemicals. Besides, these Au-based sensors show some inefficient sensing responses and DA i.e., they are small values [8,9]. In order to achieve enhanced sensitivity of a biosensor device, the desirable parameters are the better DA and the more stability than the conventional biosensors. Here, we have proposed different kinds of metal-MoS_2 and metal-Perovskite LRSPR biosensors. The sensing behaviors of the proposed biosensors have been studied. Moreover, we have also compared the optical responses of metal-graphene, metal-MoS_2 and metal-Perovskite LRSPR biosensors. The Perovskite ($CH_3NH_3PbBr_3$) material has unique feature of its outstanding photoelectric, thermal and electrical properties. So, Perovskite materials are widely used in solar cells, photoluminescence converters, microwire lasers, and other fields. Consequently, $CH_3NH_3PbBr_3$ Perovskite has used in the field of optical LRSPR sensors. Wu et al. investigated the sensitivity of the LRSPR biosensor with cytop/Al/graphene configuration and found that the sensitivity is enhanced greatly by the introduction of the graphene layer in the LRSPR biosensor configuration [10].

The present dissertation is divided into three chapters as follows:

Chapter 1 contains the basics of optics and general theories of optics. The optical density or refractive index (RI) is described with the help of Maxwell's equations. The propagation of the electromagnetic wave is considered as the light i.e. the quanta of the electromagnetic wave. The periodic structure of the RI of different materials is called photonic crystals and such crystals have unique properties i.e. called photonic band gaps. The photonic band gaps are able to control the electromagnetic waves from microwave to visible when the unit cells of the periodic dielectric materials are equivalent to the incidence wave. So, photonic crystals are used in several applications like optical sensors, biosensors, switches, reflectors, optical filters, etc. Researchers have studied the optical biosensors based on photonic crystals because optical sensors are ultra-compact size with high accuracy and

high efficiency. But the metallic photonic crystals are used for biosensors due to having surface plasmon properties in the metallic and dielectric interfaces. We have literature reviewed several papers in the field of the biosensors based on photonic crystals and we have found that the high-performance sensing behavior of biosensors based on photonic crystals can be achieved by surface plasmon resonance (SPR) and long-range surface plasmon resonance (LRSPR) because when the metal and dielectric materials are arranged in the Kretschmann configurations. The Kretschmann configuration of cytop/Al/graphene configuration based on SPR and LRSPR for biosensor applications are studied and verified theoretically [26,30,31] using transfer matrix method for TM mode. The reflectance of the considered configurations for designed biosensors investigates sensitivity, full width at half maximum and detection accuracy with the variation of optical parameters of the structure as well as the parameters of the materials. On the basis of the calculation of sensitivity, detection accuracy, and efficiency, we propose a high-performance sensing behavior of biosensors based on photonic crystals having SPR and LSPR properties.

The theory and methodology for the periodic structure of metal-dielectric materials are given in the **Chapter 2**. We have started Maxwell's equations to formalize the Master equation for Photonic Crystals (PCs) and calculate the dispersion relation for PCs using Bloch's waves. We have also given the formulation of the transfer matrix method using the Master equation. Besides this, we have also formalized the characteristic matrix for a single layer. This single-layer matrix is able to calculate the reflection and transmission coefficients, which are equivalent to Fresnel's coefficients. This characteristic matrix may also use to formulate periodic layers by just multiplying the characteristics matrix of each layer. The reflectance of the layered materials is used to calculate the parameters of the biosensors like sensitivity, detection accuracy, and efficiency. The sensitivity and detection accuracy of the biosensor especially for SPR and LRSPR based biosensors are calculated the reflectance of the incident TM-polarized light by the application of the Transfer Matrix Method [12].

In the proposed layered structure, entire layers are aligned in the z-direction and each separate layer is well-defined by their d_k thinness, n_k refractive index (RI) and ε_k dielectric constant, where k=1,2,3. The tangential EM fields at the initial boundary are fixed as

$Z=Z_1=0$; and the relation of tangential EM fields between initial and final boundary $Z=Z_{n-1}$ is followed as [14];

$$\frac{U_1}{V_1} = M \frac{U_{n-1}}{V_{n-1}} \tag{4}$$

where V_1 and U_1 are magnetic and electric fields at the boundary of the initial layer, V_{n-1} and U_{n-1} are magnetic and electric at the boundary of n^{th} layer, respectively, also M is the total product of all transfer matrices of the collective n layers in the device construction. The TMM is used for TM-polarization light and the total matrix M for considered configuration is specified as [15,16];

$$M = \prod_{k=2}^{N-1} M_k = \begin{bmatrix} M_{11} & M_{12} \\ M_{21} & M_{22} \end{bmatrix} \tag{5}$$

with

$$M_k = \begin{bmatrix} cos\beta_k & \frac{-isin\beta_k}{q_k} \\ -iq_k sin\beta_k & cos\beta_k \end{bmatrix} \tag{6}$$

where

$$q_k = \frac{(\varepsilon_k - n_1^2 sin^2\theta_1)^{1/2}}{\varepsilon_k} \text{ and } \beta_k = \frac{2\pi d_k (\varepsilon_k - n_1^2 sin^2\theta_1)^{1/2}}{\lambda},$$

Here, θ_1 is the angle of incidence of electromagnetic wave on the base of 2S2G glass prism. Using TMM, and we can obtain four elements of electric and magnetic fields in the characteristic's matrix M for periodic layers; M_{11} M_{12} M_{21} and M_{22}. By application of these essentials' components, we can compute the coefficient of total reflection r_p for TM or p-polarization light and the relation is given as follows [17];

$$r_p = \frac{(M_{11} + M_{12} q_n) q_1 - (M_{21} + M_{22} q_n)}{(M_{11} + M_{12} q_n) q_1 + (M_{21} + M_{22} q_n)} \tag{7}$$

Lastly, the reflectance R_p of n layers for p-polarization is calculated by;

$$R_p = |r_p|^2 \tag{8}$$

The variation in the n_s RI of the sensing medium can lead to alteration in reflectance R and the maximum change in R can yield a maximum sensitivity (S). Therefore, the sensitivity (S) can be defined as follows;

$$S = \frac{dR_p}{dn_s} \tag{9}$$

Now, for the proposed SPR sensor we can obtain the detection accuracy (DA) from the resulting reflective curves using full width at half maximum (FWHM) from the reflectance of the layered materials [18];

$$DA = \frac{1}{FWHM} \tag{10}$$

From equation (2.67) it is predicated that to get the maximum performance sensor, the DA must be maximum as possible. It is apparent that the detection accuracy is inversely proportion to FWHM, consequently, a finer FWHM will produce a maximum DA.

Chapter 3 contains the designed structure of the LRSPR biosensor with a thick film of Cytop of thickness of 2000 nm is shown in Fig.1 with various configurations of biosensors like Cytop/Al/graphene, Cytop/Al/MoS_2 and Cytop/Al/Perovskite with biomolecular recognition component as a sensing medium. All configurations are mounted on the chalcogenide glass (2S2G) prism. Al metal thin film of thickness 15 nm is embedded between Cytop and graphene or MoS_2 or Perovskite material. Here, the 2S2G glass with the high refractive index of has been used as the coupling prism. The employed excitation light wavelength (λ) for the LRSPR sensing is 633nm. Especially, the thickness of graphene is taken (d) i.e., d= N x 0.34 nm, where N means number of monolayers of graphene films. In our study, the thicknesses of MoS_2 and perovskite are taken the same as the thickness of the graphene. The TM-polarized electromagnetic (EM) wave is incident on one adjacent side of the 2S2G glass prism and after excitation of the EM wave with the considered configurations; the resultant reflective EM wave is detected on the same side through a photodetector i.e., ATR method Kretschmann configuration [10].

The refractive index (n_1) of the 2S2G prism is taken as [11];

$$n_1 = 2.24047 + \frac{2.693\times10^{-2}}{\lambda^2} + \frac{8.08\times10^{-3}}{\lambda^4} \tag{11}$$

where λ is understand for wavelength of incident EM wave in micrometers. Subsequent, the sensing medium of n_s=1.33 at λ=633 nm is considered due to the very small difference between RI of Cytop thin-layer (n_c=1.34), and such periodic arrangement leads to excite

LRSPPs in the metallic interface. Furthermore, the dielectric constant of the Al metal layer is, according to the Drude–Lorentz model, given as [12];

$$\varepsilon_m = 1 - \frac{\lambda^2 \lambda_c}{\lambda_p{}^2(\lambda_c + i\lambda)} \tag{12}$$

where λ_p and λ_c denote the wavelengths of plasma and collision respectively. The values of λ_p and λ_c for aluminum (Al) are 1.0657×10^{-7}m and 2.4511×10^{-5}m respectively. The RI of graphene in observable range is specified by the formula [13] that is given as;

$$n_g = 3.0 + iC_1\lambda/3; \tag{13}$$

where $C_1 \approx 5.446$ um^{-1}, while λ is the vacuum wavelength in micrometers.

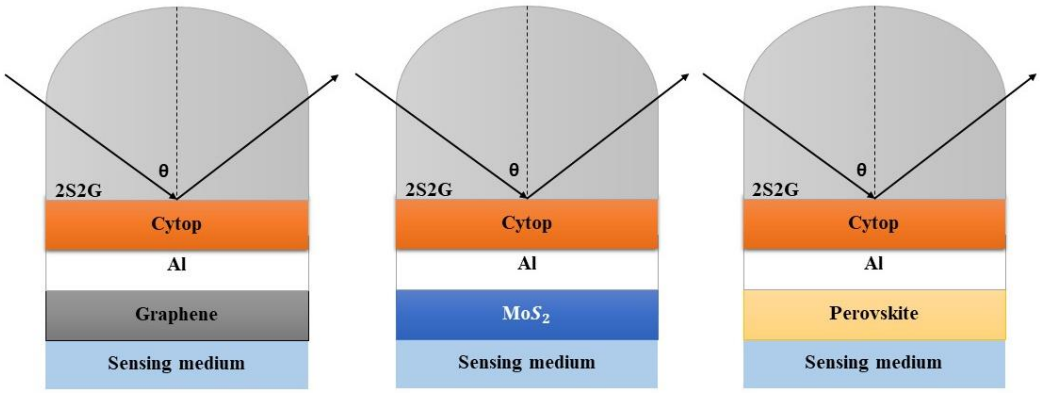

(a) (b) (c)

Figure 1: Schematic diagram of LRSPR biosensors with configurations of (a) cytop/Al/graphene, (b) cytop/Al/MoS_2 and (c) cytop/Al/Perovskite.

For our calculation convenience, we have taken the complex refractive index of MoS_2 and $CH_3NH_3PbBr_3$ Perovskite is 5.2227+1.0804*i and 2 + 0.003*i at λ = 633nm respectively [19-23]. The fluorine-containing insulating polymer, poly-perfluoro-butenyl-vinyl-ether (called Cytop), is used as a small refractive index (RI) layer in the LRSPR sensor [24]. The Cytop is an amorphous material and transparent fluoropolymer through maximum solubility and the film-forming virtues of Cytop at room temperature is also frequently considered as the insulating film in field-effect transistors [25]. Furthermore, the RI of Cytop is taken 1.34 (n_1) at λ = 633 nm, which is extensively used as matching film in SPR sensor [26].

The reflectance (R), sensitivity (S), detection accuracy (DA) and other properties of designed structure at different parameters are studied. Firstly, we have studied the reflectance and sensitivity properties by using the TMM for TM mode. Secondly, we have studied the variation of reflectance with the variation of RI of sensing medium. The FWHM and DA of the considered configurations have studied lastly.

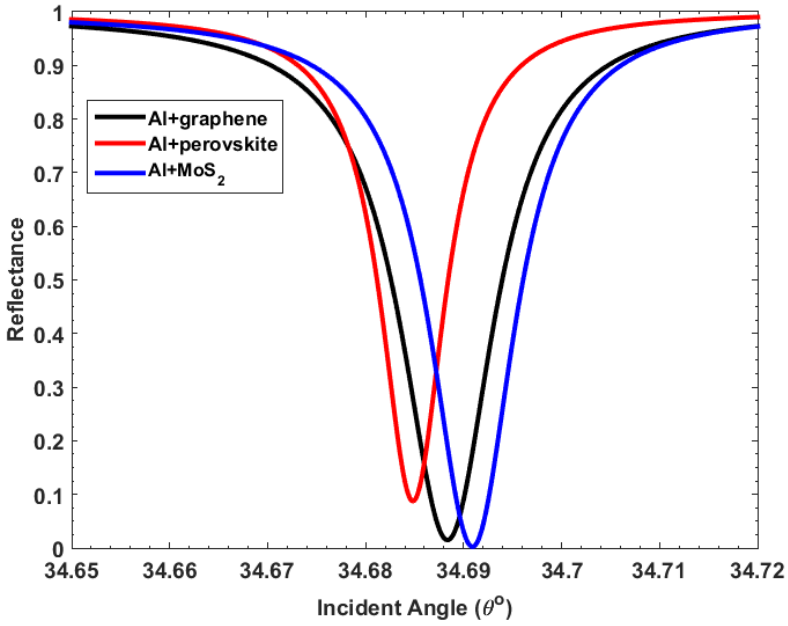

Figure 2: Reflectance of the designed biosensors as a function of incident angle for the configurations of Al+different materials.

The reflectance and sensitivity of designed structure are calculated by using TMM method for EM wave with wavelength 633 nm and RI of sensing medium n_s=1.33. Fig. 2 shows the variation of reflectance vs. incident angle for different biosensor configurations. The reflectance of Al based sensors for all combinations (Al-graphene or Al-MoS_2 or Al-Perovskite) are compared. The black curve shows the variation of reflectance regarding incident angle for combination of Aluminum-graphene layer as a conventional LRSPR optical biosensor. The red curve and blue curve show the variation of reflectance versus incident angles for corresponding Al-Perovskite layer and Al-MoS_2 layer configurations respectively. In comparison of the all reflectance, the reflectance for Al-MoS_2 is found zero at the 34.692^o resonance angle and this is most fruitful and suitable configuration for high efficiency and high accuracy LRSPR biosensor.

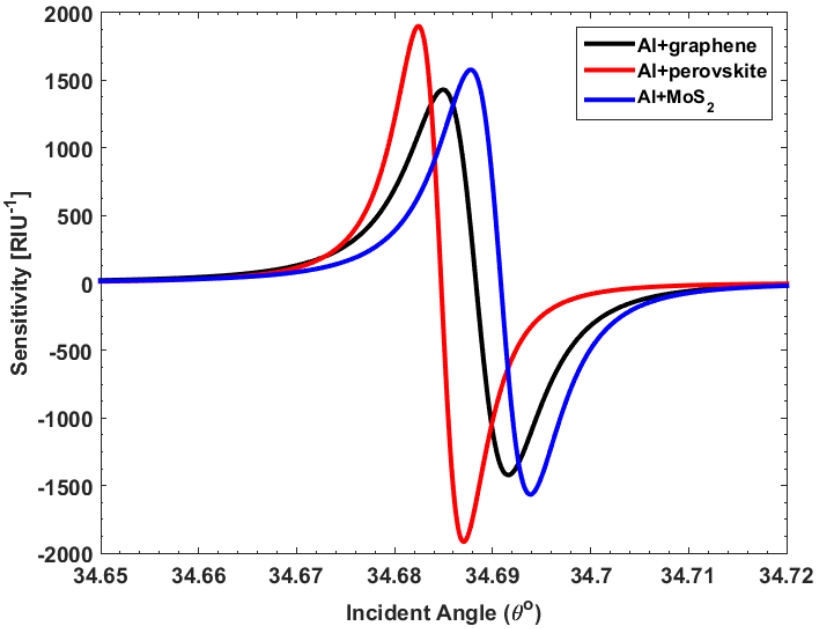

Figure 3: Sensitivity of the designed biosensors as a function of incident angle for the configurations of Al+different materials.

In Fig. 3, the sensitivity versus incident angle has been shown, the black, red and the blue curves represent the sensitivity of Al-graphene, Al-Perovskite and Al-MoS_2 layers, respectively. Depending on the surroundings and angle of incidence the peak sensitivity for the configuration of Al-graphene layer is found to be 1430 RIU^{-1} at 34.69^o resonance angle. Similarly, peak sensitivity for the configuration of Al-Perovskite and Al-MoS_2 layers are found to be 1857.6 RIU^{-1} at 34.68^o resonance angle and 1571.6 RIU^{-1} at 34.69^o resonance angle respectively. From the above results, it is evident that the proposed LRSPR biosensors with the configuration of Al metal layer and Perovskite layer combination have higher peak sensitivity in comparison to the others LRSPR biosensor configurations. The reflectance at 633 nm wavelength is studied with the variation of n_s for all configurations.

Fig. 4 shows the variation of peak sensitivity versus RI of sensing medium n_s. The black curve, the blue curve and the red curve are the variation of peak sensitivity of Aluminum-graphene, Aluminium-MoS_2 and Aluminum-Perovskite respectively with thickness of Aluminum is fixed i.e., 15nm and thicknesses of other materials are taken equivalent to single layer graphene i.e., 0.34 nm. Here, it is inferred that the peak sensitivity for graphene, MoS_2 and Perovskite layer is increased by n_s; but the sensitivity of Perovskite layer, in

comparison to both materials, is increased sharply by increasing n_s and found to be the maximum value 5220 RIU^{-1} at 34.87° for n_s =1.3425.

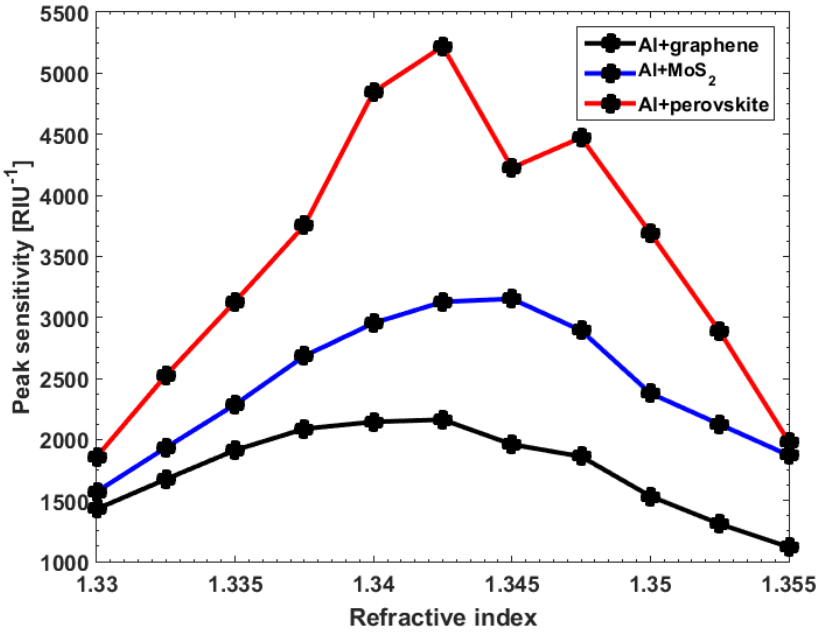

Figure 4: Peak sensitivity vs. refractive index of sensing medium for all configurations

After this maximum value of the sensitivity, it starts to decrease. This result reveals that the peak sensitivity of the Al-Perovskite configuration has best for the sensing medium of refractive index around 1.3425. A comparative table 1 for sensitivity of the biosensor with different configurations is given and indicates that the sensitivity of proposed Al-MoS_2 and Al-Peroskite based LRSPR biosensors has found nearly 10% and nearly 30% more sensitive than the standard Al-graphene LRSPR biosensor.

Table 1: Comparative table for sensitivity of the biosensor with different configurations

Configuration	Sensitivity	Reference
Al + perovskite	1857.6 RIU^{-1}	Our result [31]
Al + MoS_2	1571.6 RIU^{-1}	Our result [31]
Al + graphene	1430.0 RIU^{-1}	[18]

Graphene/Ag-based SPR sensor	455.4 RIU^{-1}	[27]
TMDCs/Al-based SPR sensor	895.6 RIU^{-1}	[28]
TMDCs/Au-based LRSPR biosensor	1240.2 RIU^{-1}	[29]

In this dissertation work, we have proposed a new configuration of LRSPR biosensors based on the Al-MoS_2 and Al-Perovskite. The proposed confugations have found the enahanced sensitivity and high detection accuracy in comparison to conventional Al-graphene LRSPR biosensor. However, the sensitivity of proposed LRSPR biosensor based on the Al-Perovskite with thickness of Perovskite material 0.34 nm has highest peak sensitivity (4847 RIU^{-1}) for sensing medium of RI 1.34, which is highest value for the LRSPR biosensors. Moreover, the sensitivity of proposed Al-MoS_2 based LRSPR biosensor is nearly 10% more sensitive than the standard Al-graphene LRSPR biosensor, while Al- Perovskite based with same congiuration type have nearly 30% more sensitive than the standard Al-graphene LRSPR biosensor.

The calculated results reveal that the enhanced sensitivity of nearly 30% Al-Perovskite and nearly 10% Al-MoS_2 based LRSPR biosensors more than the conventional Al-graphene LRSPR biosensor may be used for high performance sensing devices. Hence, the proposed LRSPR bisosensors may be useful to detect biomolecules as well as surface plasmon resonance imaging (SPRI). The SPRI may be used in several applications of biomedical, proteomics, genomics and bioengineering fields. In future, the high performance sensing devices of Al-Perovskite based LRSPR bisosensor and Al-MoS_2 based LRSPR bisosensor may be fabricated for practical realization to biomolecules detecting as well as surface plasmon resonance imaging by low cost synthesis or fabrication methods.

REFERENCES

[1] A. Ghatak, Optics, Tata McGraw-Hill, New Delhi, 2008.

[2] D. J. Griffiths, Introduction to Electrodynamics, Prentice Hall, Upper Saddle River, New Zersey, USA, 1999.

[3] P. Yeh, Optics in Layered Media, John Willey and Sons, New York, 1988.

[4] Y. Fink, J. N. Winn, S. Fan, C. Chen, J. Michel, J. D. Joannopoulos, E. L. Thomas, A dielectric omnidirectional reflector, Science 282, 1679–1682, 1998.

[5] H. Inan, M. Poyraz, F. Inci, M. A. Lifson, M. Baday, B.T. Cunningham, U. Demirci, Photonic crystals: emerging biosensors and their promise for point-of-care applications, Chem. Soc. Rev. 46, 366–388, 2017.

[6] D. Sarid, Long-Range Surface-Plasma Waves on Very Thin Metal Films, Phys. Rev. Lett., 47, 1927–1930, 1981.

[7] K. Matsubara, S. Kawata, S. Minami, Multilayer system for a high-precision surface plasmon resonance sensor, Opt. Lett., 15, 75–77, 1990.

[8] O. Krupin, H. Asiri, C. Wang, R. N. Tait. P. Berini, Biosensing using straight long-range surface plasmon waveguides, Opt. Exp., 21, 698–709, 2013.

[9] J. C. Love, L. A. Estroff, J. K. Kriebel, R. G. Nuzzo, G. M. Whitesides, Self-assembled monolayers of thiolates on metals as a form of nanotechnology, Chem. Rev., 105, 1103–1169, 2005.

[10] L. Wu, Z. Ling, L. Jiang, J. Guo, X. Dai, Y. Xiang, D. Fan, Long-Range Surface Plasmon With Graphene for Enhancing the Sensitivity and Detection Accuracy of Biosensor, IEEE Photonics J., 8, 4801409, 2016.

[11] P. K. Maharana, R. Jha, Chalcogenide prism and graphene multilayer based surface plasmon resonance affinity biosensor for high performance, Sensors and Actuators: B. Chem., 169, 161–166, 2012.

[12] A. K. Sharma, B. D. Gupta, On the performance of different bimetallic combinations in surface plasmon resonance based fiber optic sensors, J. Appl. Phys., 101, 093111, 2007.

[13] M. Bruna, S. Borini, Optical constants of graphene layers in the visible range, Appl. Phys. Lett., 94, 031901, 2009.

.

[14] S. Zeng, S. Hu, J. Xia, T. Anderson, X-Q. Dinh, X-M. Meng, P. Coquet, K-T. Yong, Graphene-MoS_2 hybrid nanostructures enhanced surface plasmon resonance biosensors, Sensors and Actuators: B. Chem., 207, 801–810, 2015.

[15] P. K. Maharana, R. Jha, S. Palei, Sensitivity enhancement by air mediated graphene multilayer-based surface plasmon resonance biosensor for near infrared, Sensors and Actuators: B. Chem., 190, 494–501, 2014.

[16] R. Verma, B. D. Gupta, R. Jha, Sensitivity enhancement of a surface plasmon resonance-based biomolecules sensor using graphene and silicon layers, Sensors and Actuators: B. Chem., 160, 623–631, 2011.

[17] L. Wu, H. S. Chu, W. S. Koh, E. P. Li, Highly sensitive graphene biosensors based on surface plasmon resonance, Opt. Express, 18, 14395–14400, 2010.

[18] P. K. Maharana, T. Srivastava, R. Jha, On the performance of Highly Sensitive and Accurate Graphene-on-Aluminum and Silicon-Based SPR Biosensor for Visible and Near Infrared, *Plasmonics*, 9 (5), 1113–1120, 2014.

[19] J. B. Maurya, A. Francois, Y. K. Prajapati, Two-Dimensional Layered Nanomaterial-Based One Dimensional Photonic Crystal Refractive Index Sensor, Sensors, 18, 857, 2018.

[20] https://refractiveindex.info/?shelf=main&book=MoS2&page=Beal, 2022.

[21] A. R. Beal, H. P. Hughes, Kramers-Kronig analysis of the reflectivity spectra of 2H-MoS_2, 2H-$MoSe_2$ and 2H-$MoTe_2$. J. Phys. C: Solid State Phys. 12, 881–890, 1979.

[22] S. Brittman, E. C. Garnett, Measuring n and k at the Microscale in Single Crystals of $CH_3NH_3PbBr_3$ Perovskite, J. Phys. Chem. C 120, 616–620, 2016.

[23] H. Zhang, Y. Ma, Y. Wan, X. Rong, Z. Xie, W. Wang, L. Dai, Measuring the refractive index of highly crystalline monolayer MoS_2 with high confidence, Sci. Rep. 5, 8440, 2015.

[24] Y. Zheng, W. Shi, J. Kong, D. Huang, H. E. Katz, J. Yu, A. D. Taylor, A Cytop Insulating Tunneling Layer for Efficient Perovskite Solar Cells, Small Methods 1, 1700244, 2017.

[25] W. Huang, K. Besar, R. LeCover, P. Dulloor, J. Sinha, J. F. M. Hardigree, C. Pick, J. Swavola, A. D. Everett, J. Frechette, M. Bevan, H. E. Katz, Label-free brain injury

biomarker detection based on highly sensitive large area organic thin film transistor with hybrid coupling layer, Chem. Sci. 5, 416–426, 2014.

[26] C. Yue, Y. Lang, X. Zhou, Q. Liu, Sensitivity enhancement of an SPR biosensor with a graphene and blue phosphorene/transition metal dichalcogenides hybrid nanostructure, Appl. Opt. 58, 9411-9420, 2019.

[27] P. K. Maharana, R. Jha, P. Padhy, On the electric field enhancement and performance of SPR gas sensor based on graphene for visible and near infrared, Sensors and Actuators: B. Chem., 207, 117-122, 2015.

[28] Y. Xu, L. Wu, L. K. Ang, MoS_2 Based Highly Sensitive Near-Infrared Surface Plasmon Resonance Refractive Index Sensor, IEEE J. Selected Topics Quant. Electronics, 25, 2, 1-7, 2019.

[29] Y. Xu, C-Y. Hsieh, L. Wu, L. K. Ang, Two dimensional transition metal dichalcogenides mediated long range surface plasmon resonance biosensors, J. Phys. D, 52, 6, 065101, 2019.

[30] Q. Wang, J-Y. Jinga, Z. Cheng, Long-range surface plasmon resonance and its biological sensing applications, Chapter-Eight, Handbook on Comprehensive Analytical Chemistry, 95, 277-338, 2021, ISBN 9780323853095; https://www.sciencedirect.com/science/article/abs/pii/S0166526X21000726.

[31] M. Kumar, K. B. Thapa, P. Singh, Long-range surface plasmon resonance biosensors with cytop/Al/Perovskite and cytop/Al/MoS_2 configurations, Phys. Scr., 97, 055501, 2022.